A Characteristic Scale in Radiation Fields of Fractal Clouds

W. Wiscombe, R. Cahalan, A. Davis, and A. Marshak
National Aeronautics and Space Administration/Goddard Space Flight Center
Climate & Radiation Branch
Greenbelt, Maryland

The wavenumber spectrum of Landsat imagery for marine stratocumulus clouds shows a scale break when plotted on a double log plot; the ≈–5/3 slope is interrupted at a scale around 200 m and followed by a much steeper slope (Cahalan and Snider 1989). We offer an explanation of this scale break in terms of a smoothing by horizontal radiative fluxes (Davis et al. 1995), which is parameterized and incorporated into an improved independent pixel approximation (Marshak et al. 1995).

We compute the radiation fields emerging from cloud models with horizontally variable optical depth fields given by fractal models developed by Schertzer and Lovejoy (1987), Cahalan et al. (1994), and Marshak et al. (1994). These models were tuned to have spectral exponents around 5/3, as observed by Cahalan and Snider (1989) using ground-based microwave radiometry. Two approaches were used: 1) the independent pixel approximation (IPA) which treats the radiation properties of each pixel as a 1-D plane-parallel layer, ignoring any net horizontal transport; and 2) forward Monte Carlo (MC) simulation with variance reduction. For marine stratocumulus, IPA and MC have close domain-average albedoes (Cahalan et al. 1994), but there are dramatic differences in individual pixel values. Figure 1 illustrates the random optical depth field and the two albedo fields calculated by IPA and MC methods.

We use comparative spectral and multifractal analyses to qualify the validity of the IPA at the largest scales and demonstrate its shortcomings on the smallest scales. We show that there is a characteristic scale η_{rs} which we call the "radiative smoothing scale." For scales smaller than η_{rs}, the IPA follows the fluctuations of the optical depth field whereas the MC albedo has a much smoother behavior with a spectral exponent around 3 (Figure 2). For scales larger than η_{rs}, IPA and MC albedoes and nadir radiances have similar spectral properties which resemble those of the optical depth field. Multifractal properties differ only for the higher moments (Davis et al. 1994) implying that, the bigger the jumps in optical depth, the more powerful the radiative smoothing.

The location η_{rs} of the scale break is determined entirely by the characteristic size $\langle\xi\rangle$ of the spot resulting from localized illumination. The size of this spot is shown to be proportional to the harmonic mean of the product of the transport mean free path and the geometrical cloud thickness, h, in the frame of diffusion theory for homogeneous media. Equivalently,

$$\langle\xi\rangle \approx \frac{h}{\sqrt{(1-g)\,\tau}} \qquad (1)$$

where τ is the cloud optical thickness and g is the asymmetry factor. Numerical calculations show that Equation (1) remains true for fractal cloud models with τ replaced by its average value $\langle\tau\rangle$. Typical values for marine Sc are h = 0.3 km, $\langle\tau\rangle$ = 13, and g = 0.85, so that $\langle\xi\rangle \approx$ 0.2 km.

If the shape and size of the spot are known, then the effect of the horizontal photon transport can be estimated. More precisely, IPA fields can be corrected by convolution with the probability density function describing the spot. The shape of the spot, meaning the distribution of the distance ξ between photon entry- and exit-points, is well approximated by a gamma-type distribution for both homogeneous and fractal models:

$$\rho(\alpha,\langle\xi\rangle;\xi) = \frac{1}{\gamma(\alpha)}\left(\frac{\alpha}{\langle\xi\rangle}\right)^{\alpha}\xi^{\alpha-1}\,e^{-\alpha\xi/\langle\xi\rangle}$$
$$\text{with } \alpha = \left(\frac{\langle\xi^2\rangle}{\langle\xi\rangle^2} - 1\right)^{-1} \qquad (2)$$

The improved "nonlocal" IPA albedo,

$$R_{NIP}(\chi) = \frac{1}{2}\int_{-\infty}^{\infty} R_{IP}(\chi')\,\rho(\alpha,\langle\xi\rangle;|\chi-\chi'|)\,d\chi' \qquad (3)$$

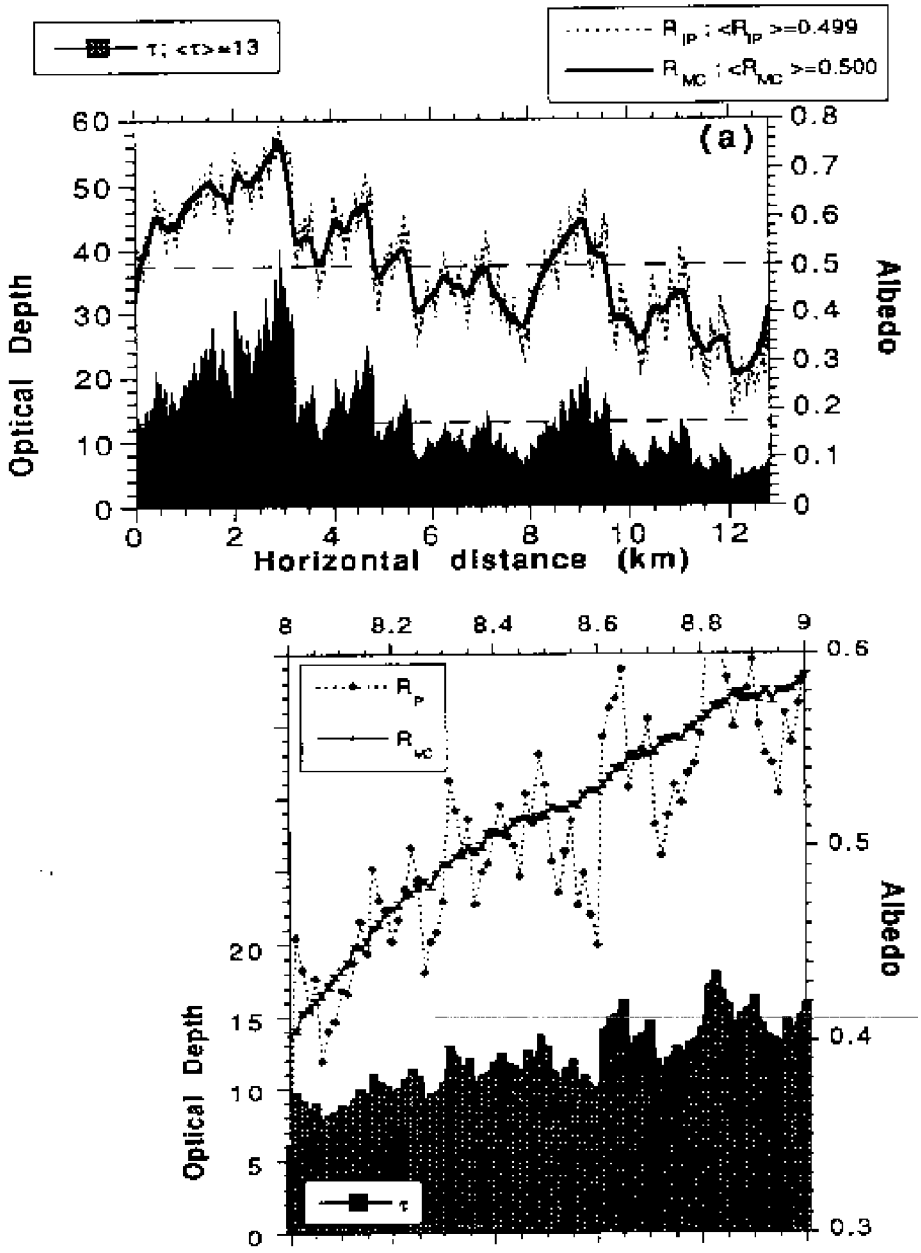

Figure 1. Horizontal variations of optical depth, IPA and MC albedoes. (a) The lower curve is optical depth simulated by a fractal bounded cascade model with 10 cascade steps and $\langle\tau\rangle$=13 (left axis); the two upper curves are the IPA and MC albedo fields (sun angle θ=22.5°, asymmetry factor g=0.85). Geometrical thickness h = 300 m, horizontal pixel size is 12.5 m. The basic cloud element is 0.3 km thick and 2^{10}x12.5 $10^3 \approx$12.8 km long (there is no variability in the y direction). MC and IPA yield almost equal domain-average albedo 0.5 but they show radically different degrees of smoothness (the thickness of the MC curve shows the level of its numerical noise). (b) A one km zoom of panel (a) where the MC noise is now visible.

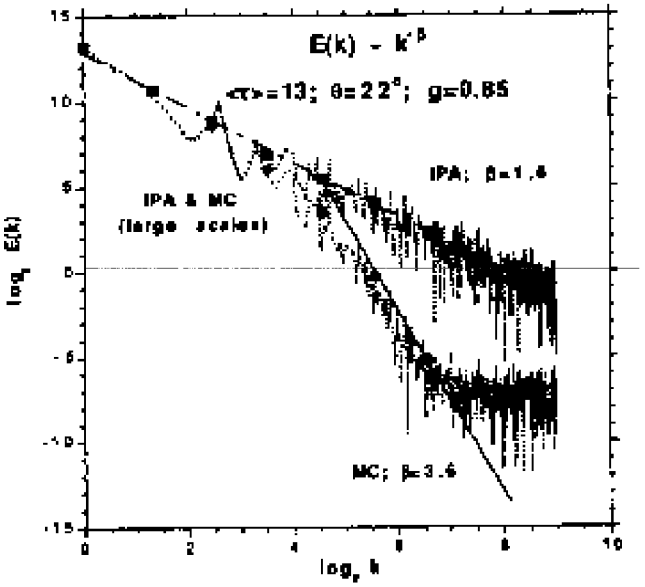

Figure 2. Energy spectra of IPA- and MC-simulated albedo fields. Parameters are the same as in Figure 1.

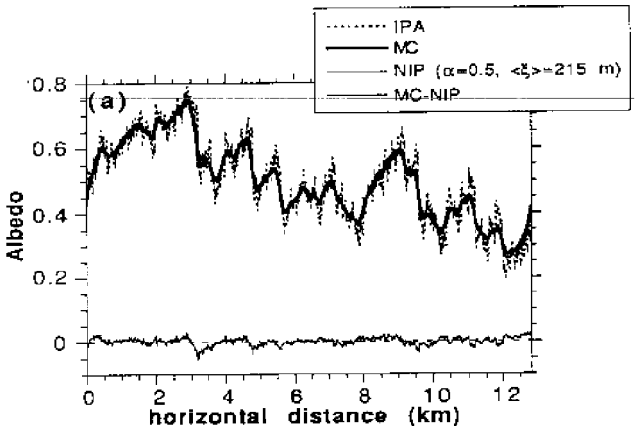

Figure 3. Nonlocal independent pixel approximation. Fractal model for optical depth is the same as in Figure 1. Three albedo fields calculated by the IPA, MC, and the improved IPA in Equation (3) are presented. The first two fields are the same as in Figure 1. The lower curve shows the differences between MC and the new "nonlocal" IPA.

generates smoother fields at small scales and leaves large-scale properties unchanged (Marshak et al. 1995). To approximate the MC albedo results in Figure 1 starting with the IPA, we take $p(\alpha,\langle\xi\rangle;\xi)$ with $\alpha = 1/2$ for simplicity and $\langle\xi\rangle = 0.215$ km from Equation (1). In Figure 3 we plotted the three albedo fields (R_{IP}, R_{MC} and R_{NIP}) highlighting the small residuals between R_{MC} and R_{NIP}.

If the wavenumber spectrum E(k) of cloud liquid water (and, hence, that of the associated IP) follows the $k^{-5/3}$ power law, convolution with the spot shape yields a field with a spectrum

$$E(k) \sim k^{-5/3} \frac{\cos^2\left[\alpha \tan^{-1}\left(k\langle\xi\rangle/\alpha\right)\right]}{\left[1 + \left(k\langle\xi\rangle/\alpha\right)^2\right]^{\alpha}} \qquad (4)$$

For scales larger than $\langle\xi\rangle$, we find both cloud liquid water and albedo have the same scaling behavior, while for scales less than $\langle\xi\rangle$, the albedo is much smoother, in agreement with analyses of Landsat observations of marine Sc by Cahalan and Snider (1989) and with our accurate MC results.

References

Cahalan, R. F., and J. B. Snider. 1989. Marine stratocumulus structure, *Remote Sens. Environ.*, **28**, 95–107.

Cahalan, R. F., W. Ridgway, W. J. Wiscombe, T. L. Bell, and J. B. Snider. 1994. The albedo of fractal stratocumulus clouds, *J. Atmos. Sci.*, **51**, 2434–2455.

Davis, A., A. Marshak, W. Wiscombe, and R. Cahalan. 1994. Multifractal characterizations of non-stationarity and intermittency in geophysical fields, observed, retrieved, or simulated, *J. Geophys. Res.*, **99**, 8055–8072.

Davis, A., A. Marshak, and W. Wiscombe. 1995. A horizontal radiative flux in stratocumulus and the landsat scale-break, *J. Atmos. Sci.*, submitted.

Marshak, A., A. Davis, R. Cahalan, and W. Wiscombe. 1994. Bounded cascade models as nonstationary multiractals, *Phys. Rev. E*, **49**, 55–69.

Marshak, A., A. Davis, W. Wiscombe, and R. Cahalan. 1995. Radiative smoothing in fractal clouds, *J. Geophys. Res.*, **100**, 26247-26261.

Schertzer, D., and S. Lovejoy. 1987. Physical modeling and analysis of rain clouds by anisotropic scaling multiplicative processes, *J. Geophys. Res.*, **92**, 9693–9714.